Submitted to CRATER - Conference on Recent Advances in Translational Eye Research 2025

Hyperspectral imaging, phasor analysis and deep learning for ocular diagnosis

Meritxell Vilaseca*, Francisco J. Burgos, Laura Rey, Armin Eskandarinasab, Marina Bou & Fernando Díaz-Doutón

Center for Sensors, Instruments and Systems Development (CD6), Universitat Politècnica de Catalunya (UPC), Rambla Sant Nebridi 10, 08222 Terrassa-Barcelona, Spain
#corresponding author email: meritxell.vilaseca@upc.edu

1. Introduction

Hyperspectral imaging has emerged as a powerful tool for diagnostic applications in medicine, offering both spectroscopic and morphological information critical for analysing biological samples. Its integration with advanced deep learning algorithms holds significant promise for transforming medical diagnostics in the coming years. In this talk, we will present our latest advancements in these areas, focusing on improving the diagnosis of various eye diseases [1, 2].

Firstly, we describe a multiplexed staring hyperspectral fundus camera developed to improve non-invasive diagnosis of eye fundus diseases. This system incorporates both silicon and InGaAs sensors, along with light-emitting diodes (LEDs), enabling the acquisition of visible and near-infrared images of eye fundus structures. These images capture spectral signatures unique to different components of biological tissue, enhancing diagnostic capability.

To address the high dimensionality and potential redundancy of hyperspectral data, we apply a phasor analysis approach [3,4]. This method, effective in a range of fields involving complex datasets, projects high-dimensional spectral data onto a two-dimensional plane. This facilitates data interpretation while preserving essential information about the fundus, even in the presence of inter-band correlation.

Finally, we explore the use of computer-aided diagnosis based on customized machine and deep learning algorithms to process spectral fundus image cubes [5]. These models are trained to distinguish between healthy and diseased retinal samples using hyperspectral data, rather than traditional RGB color images. This marks a significant advancement in ocular diagnostics, highlighting the importance of combining spatial and spectral information, particularly of wavelengths beyond the visible range.

2. Methods and results

Hyperspectral images acquired using a custom-built, area-scanning hyperspectral retinograph will be presented (see [2] for further details). The system features an optical setup with an array of LEDs, each emitting light at a specific peak wavelength, and two cameras: a high-resolution CMOS sensor (2048 × 2048 pixels, 6.5 μm pixel size, 16-bit depth) capturing 12 spectral bands from 416 to 955 nm, and a lower-resolution InGaAs camera (640 × 512 pixels, 20 μm pixel size, 14-bit depth) capturing three bands from 1025 to 1213 nm. The inclusion of near-infrared wavelengths, in addition to visible light, enables imaging of deeper retinal layers such as the choroid—structures typically inaccessible with conventional color fundus cameras.

Using this device, a spectral image database was built from 305 retinas (60 diseased and 245 healthy). Pathologies in the diseased group included Age-related Macular Degeneration (AMD), epiretinal membrane, and retinal detachment, among others. Images were collected at the Instituto de Microcirugía Ocular (IMO - Miranza Group, Barcelona, Spain) and the Vision University Center (CUV) of the Universitat Politècnica de Catalunya (Terrassa, Spain) [1].

Phasor analysis was applied to a subset of 102 retinas. For each pixel in the hyperspectral cube (x, y, λ), the spectral data were represented as a complex number with real and imaginary components ($g_{x,y} + is_{x,y}$) and processed using a discrete Fourier transform [3,4] (see Fig. 1). The resulting averaged phasor representations served as input for several machine learning classifiers—such as Gaussian Naive Bayes (GNB), Support Vector Machine (SVM), and ν-SVM—achieving an overall classification accuracy of 89%, with a sensitivity of 94% and specificity of 85%.

Additionally, a conditional variational autoencoder (originally developed for ventricular arrhythmia prediction [6]) was fine-tuned as a screening tool for fundus pathology using spectral imaging data. This model demonstrated excellent performance, with an overall accuracy of 96%, sensitivity of 92%, and specificity of 97%. Notably, the most effective input configuration used high-resolution images within the 416–955 nm spectral range.

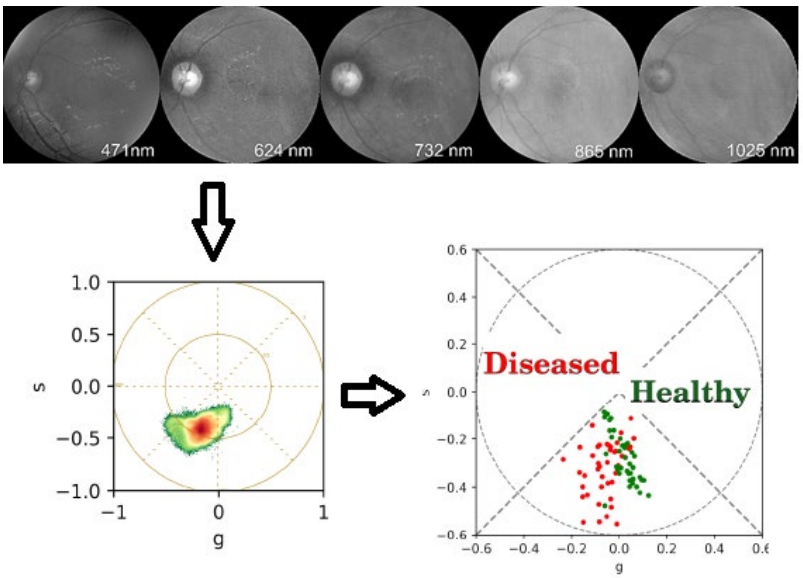

Fig. 1. Spectral images acquired for a retina (top), phasor analysis of all pixels in the images (bottom left) and average phasor analysis corresponding to the 102 retinas, allowing classification between healthy and diseased (bottom right).

Finally, we will also review other medical applications explored by our group, including the use of hyperspectral imaging combined with machine learning and deep learning algorithms for the diagnosis of skin cancer and blood disorders [7–10].

3. Acknowledgement

Funded by European Union (HORIZON–MSCA–2022–DN, GA no101119924–BE-LIGHT) and by MCIU/AEI/10.13039/501100011033 and FEDER, EU (Grant PID2023-147541OB-I00).

4. References

[1] Burgos-Fernández, F.J., Alterini, T., Díaz-Doutón, F., González, L., Mateo, C., Mestre, C., Pujol, J., Vilaseca, M. Reflectance evaluation of eye fundus structures with a visible and near-infrared multispectral camera. Biomed Opt Express 13(6), 3504-19 (2022).

[2] Alterini, T., Díaz-Doutón, F., Burgos-Fernández, F.J., González, L., Mateo, C., Vilaseca, M. Fast visible and extended near-infrared multispectral fundus camera. J Biomed Opt 24(09), 096007 (2019).

[3] Parra, A., Denkova, D., Burgos-Artizzu, X.P., et al. Metaphor: Metabolic evaluation through phasor-based hyperspectral imaging and organelle recognition for mouse blastocysts and oocytes. Proc Natl Acad Sci 121(28), e2315043121 (2024).

[4] Malacrida, L., Gratton, E., Jameson, D. M. Model-free methods to study membrane environmental probes: a comparison of the spectral phasor and generalized polarization approaches. Methods Appl Fluoresc., 3(4), 047001 (2015).

[5] Jeong, Y., Hong, Y.-J., Han, J.-H. Review of machine learning applications using retinal fundus images. Diagnostics 2022, 12, 134.

[6] Ly, B., Finsterbach, S., Nuñez-Garcia, M., Cochet, H., & Sermesant, M. Scar-related ventricular arrhythmia prediction from imaging using explainable deep learning. In International Conference on Functional Imaging and Modeling of the Heart (pp. 461-470). Cham: Springer International Publishing (2021).

[7] Rey-Barroso, L., Vilaseca, M., Royo, S., Díaz-Doutón, F., Lihacova, I., Bondarenko, A., Burgos-Fernández, F.J. Training state-of-the-art deep learning algorithms with visible and extended near-infrared multispectral images of skin lesions for the improvement of skin cancer diagnosis. Diagnostics 15(3), (355), 2025.

[8] Rey-Barroso, L., Peña-Gutiérrez, S., Yáñez, C., Burgos-Fernández, F.J., Vilaseca, M., Royo, S. Optical Technologies for the Improvement of Skin Cancer Diagnosis: A Review. Sensors 21(1), 252 (2021).

[9] Rey-Barroso, L., Roldán, M., Burgos-Fernández, F.J., Gassiot, S., Ruiz Llobet, A., Isola, I., Vilaseca, M. Spectroscopic evaluation of red blood cells of thalassemia patients with confocal microscopy: a pilot study. Sensors (Basel). 20(14), 4039 (2020).

[10] Rey-Barroso, L., Roldán, M., Burgos-Fernández, F.J., Isola, I., Ruiz Llobet, A., Gassiot, S., Sarrate, E., Vilaseca, M. Membrane protein detection and morphological analysis of red blood cells in hereditary spherocytosis by confocal laser scanning microscopy. Microsc Microanal. 29(2), 777-785 (2023).